Test Results of the ITER PF Insert Conductor Short Sample in SULTAN

P. Bruzzone, M. Bagnasco, D. Bessette, D. Ciazynski, A. Formisano, P. Gislon, F. Hurd, Y. Ilyin, R. Martone, N. Martovetsky, L. Muzzi, A. Nijhuis, H. Rajainmäki, C. Sborchia, B. Stepanov, L. Verdini, R. Wesche, L. Zani, R. Zanino, and E. Zapretilina

***Abstract*—A short sample of the NbTi cable-in-conduit conductor (CICC) manufactured for the ITER PF insert coil has been tested in the SULTAN facility at CRPP. The short sample consists of two paired conductor sections, identical except for the sub-cable and outer wraps, which have been removed from one of the sections before jacketing. The test program for conductor and joint includes DC performance, cyclic load and AC loss, with a large number of voltage taps and Hall sensors for current distribution. At high operating current, the DC behavior is well below expectations, with temperature margin lower than specified in the ITER design criteria. The conductor without wraps has higher tolerance to current unbalance. The joint resistance is by far higher than targeted.**

***Index Terms*—Cable-in-conduit conductor, ITER, joint resistance, niobium-titanium, self-field induced quench.**

I. Introduction

THE Poloidal Field Conductor Insert (PFCI) is so far the only full size demonstration project for the NbTi conductors of the ITER magnets. Based on a cable prepared in Russia, the insert coil is being manufactured in Europe and will be tested in Japan [1]. Two short conductor sections have been assembled into a short sample [2] for the SULTAN test facility [3]. A testing group, including members of many European labs as well as ITER IT members, has been entrusted with the assessment of the test results. The main aim of the test, carried out in March–May 2004, is a wide characterization of the NbTi CICC and a qualification of the joint layout for the Insert Coil.

Manuscript received October 4, 2004.

P. Bruzzone, B. Stepanov, and R. Wesche are with the EPFL-CRPP, Fusion Technology, 5232 Villigen PSI, Switzerland (e-mail: bruzzone@psi.ch; stepanov@psi.ch; wesche@psi.ch).

M. Bagnasco and R. Zanino are with the Politecnico di Torino, 10129 Torino, Italy (e-mail: maurizio.bagnasco@polito.it; roberto.zanino@polito.it).

D. Bessette is with the ITER-CTA, 85748 Garching b. München, Germany (e-mail: bessetted@itereu.de).

D. Ciazynski and L. Zani are with the CEA Cadarache, 13108 St. Paul Lez Durance, France (e-mail: daniel.ciazynski@cae.fr; louis.zani@cea.fr).

A. Formisano and R. Martone are with the Seconda Università di Napoli, 81031 Aversa, Italy (e-mail: A.Formisano@unina.it; martone@unina.it).

P. Gislon, L. Muzzi, and L. Verdini are with the ENEA, 00044 Frascati, Italy (e-mail: gislon@frascati.enea.it; muzzi@frascati.enea.it; verdini@frascati.enea.it).

F. Hurd, H. Rajainmäki, and C. Sborchia are with the EFDA, 85748 Garching b. München, Germany (e-mail: hurdf@ipp.mpg.de; hannu.rajainmaki@tech.efda.org; sborchc@ipp.mpg.de).

Y. Ilyin and A. Nijhuis are with the University of Twente, 7500 AE Enschede, The Netherlands (e-mail: Y.Ilyin@tnw.utwente.nl; A.Nijhuis@tnw.utwente.nl).

N. Martovetsky is with the LLNL, Livermore, CA 94550 USA (e-mail: martovetsky1@llnl.gov).

E. Zapretilina is with the NIIEFA, 196641 St. Petersburg, Russian Federation.

Digital Object Identifier 10.1109/TASC.2005.849084

TABLE I
LAYOUT OF THE PFIS CONDUCTORS, COMPARED TO ITER PF1&6 DESIGN

	$PFIS_W$	$PFIS_{NW}$	ITER PF1&6
NbTi strand diameter (Ni coated), mm	0.73	0.73	0.73
Cu:non-Cu	1.41*	1.41*	1.6
Number of strands (3x4x4x5x6)	1440	1440	1440
Total Cu cross section, mm^2	353	353	371
Total non-Cu cross section, mm^2	250	250	232
Sub-cable wraps cross section, mm^2	13.4	-	7.6
Outer wrap cross section, mm^2	22.3	-	19.8
Cable space diameter, mm	37.53	36.89	38.2
Cable pitches, mm	42/86/ 122/158/ 489	42/86/ 122/158/ ≈530	45/85/ 125/165/ 425
Estimated/retained cosθ	0.96	0.96	0.95
Steel spiral for central channel, mm	10 x 12	10 x 12	10 x 12
Void fraction, %	33.5**	34.3**	34.5
Outer conductor size, mm	50.35 x 50.45	49.82 x 49.78	53.8x53.8

* weighted average according to strand and cable QA sheets
** calculated assuming zero elongation of the strands during the compaction

II. Conductor and Sample Layout

Although some parameters have been a priori dictated by the availability of material (e.g. Cu:non-Cu ratio and steel jacket size), the conductor layout of the PFCI reflects the design of the ITER PF1&6 conductors [4], as shown in Table I.

A 74 m long cable section has been manufactured at VNIIKP (Podolsk, Russia) [5], based on 130 km of NbTi strand, 17 batches/126 unit lengths, supplied by Bochvar RIIM (Moscow). Based on the results of all the I_c data sheets, the supplier proposed an interpolation formula for J_c in the strand [6], marginally corrected by the testing group:

$$J_c(B,T) = C_0 B_{c2}(T)^{m-p} \times B^{p-1}(1-b)^q$$

$$B_{c2}(T) = B_{c2}(0)(1-t^2) \times (1-c_1 t)$$

where

$$b = \frac{B}{B_{c2}}(T) \qquad t = \frac{T}{T_c}$$

$B_{c2}(0)$	13.65
T_c	9.33
m	2.36
p	1.05
q	1.22
C_0	$2.899\,28 * 10^8$
c_1	0.167

The above formula is retained in the predictive analyses [7]. Another fit, based on test results of a single strand over a broader range of temperature, is reported in [8].

The jacketing into circle-in-square stainless steel tubing was carried out at Ansaldo (Italy). A 59 m long conductor section was supplied to Tesla (UK) to wind the Insert Coil. Three

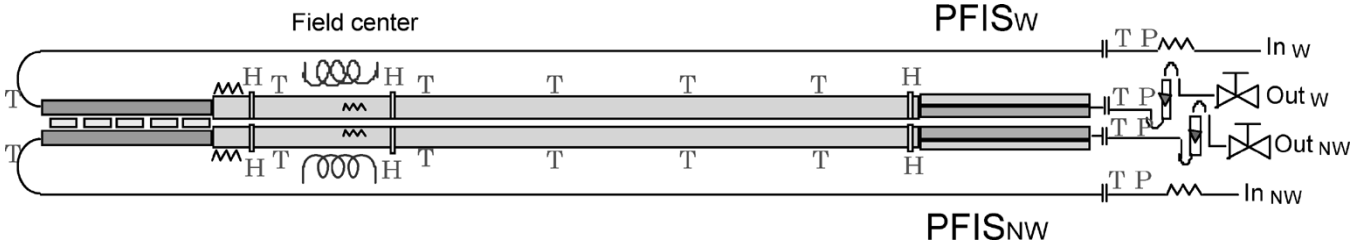

Fig. 1. Instrumentation sketch of PFIS: "H" is for the Hall sensor arrays, "T" and "P" for temperature and pressure sensors (voltage taps are not shown). The sample is positioned in vertical orientation with coolant flow from the bottom to the top.

straight sections, each about 5 m long, were also supplied. In one of the cable short section, the sub-cable and outer wraps have been removed and the jacket has been compacted to a slightly smaller size, see Table I.

The sample for SULTAN, named PFIS = Poloidal Field Insert(conductor) Sample, consists of one "regular" conductor section $(\mathrm{PFIS_W})$ and one "de-wrapped" section $(\mathrm{PFIS_{NW}})$, joined at one end by a hairpin joint, prepared by compacting the cable ends into CuCrZr sleeves and joining them by five copper saddles [2]. The Ni coating is removed from the strands in contact with the sleeve and replaced by Ag. The inner wall of the sleeve is tinned and the contact between sleeve and saddle is made by a number of indium wires, pressed by the joint clamp to a 0.2 mm thick layer.

The PFIS dimension is the standard of the SULTAN samples [9], about 3.5 m long including the hairpin joint and the upper connections. The two conductor lengths are cooled in parallel by independent circuits, with coolant flow from bottom to the top. To avoid temperature gradients over the conductor cross-section and improve the definition of the operating temperature, the central channel has been blocked in both conductor sections inserting a rubber pipe plugged at the outlet side. The central channel is free in the joint and in the termination.

The facility instrumentation, right end of Fig. 1, includes heaters, temperature and pressure sensors at inlets and mass flow meters, cryogenic valves and temperature and pressure sensors at the outlets. Ten temperature sensors are attached to the PFIS (symbol "T" in Fig. 1), nested in holes drilled in the jacket. Two sensors are in the inlet pipes, next to the joint.

Two heaters are wrapped on the conductor jacket just downstream of the joint and two small heaters, 6 mm $\times$ 20 mm, are placed in the high field region for local energy deposition.

Six arrays of Hall sensors are attached to the conductors in high field, next to the joint and termination (symbol "H" in Fig. 1) to sense the self-field distribution. The conductor jacket is turned round to a constant wall thickness at the location of the arrays. Each array includes 10 sensors. Next to the upper termination, where the stray field from the facility is weak, the sensors are symmetrically distributed over the jacket perimeter, in radial direction. At the other four locations, the 10 sensors are oriented parallel to the background field to improve the resolution of the self-field signal [10], [11]. The active spot of the sensor is placed at $\varnothing = 49\ \mathrm{mm}$, i.e. about 6.5 mm from the outer edge of the cable.

A saddle shaped pick-up coil is attached to each conductor in the high field/AC field region to detect the magnetization change, see Fig. 1. Compensation coils are placed outside the test well, next to the AC field coils.

A total of 37 voltage tap pairs are placed along and across the conductors and joint. Two synchronized data acquisition systems collect respectively 63 and 68 signal channels at 25 Hz sampling rate (AC loss runs use a higher sampling rate). The ASCII files of the two systems are imported into a single spreadsheet. The unusual large number of channels leads to very bulky files, in the range of 20–70 MB for each run.

III. Summary of Test Results

The test campaign for the PFIS lasted from mid March to the end of April 2004, with 50 critical current (I_c) and 20 current sharing temperature (T_cs) runs at various operating conditions and 100 bipolar load cycles ($\pm$45 kA @ 7 T background field). Due to the high joint resistance, the I_c runs were not isothermal and the ramp rate was not constant. The current distribution, monitored by the Hall probes for all the runs, was investigated for different current ramp rate and long holding time. An additional test campaign in September 2004 allowed accurate AC loss test by gas flow calorimetry for both conductors in the background field of 2 T, with AC field amplitude of $\pm$0.2 T.

A. DC Performance

The electric field at which the quench occurs, E_q, decreases with increasing current, as a result of the superposition of self-field and background field. The local electric field along a strand in the cable reaches very high values at the peak magnetic field, driving a quench, although the average electric field, sensed by the voltage taps on the conductor jacket remains very low. Such self-field induced, sudden take-offs are typical of large size NbTi CICC [12]–[14].

The 0.1 $\mu\mathrm{V/cm}$ criterion for I_c and T_cs test could only be measured for current below 45 kA $(\mathrm{PFIS_{NW}})$ and 38 kA $(\mathrm{PFIS_W})$. The behavior of I_c vs. temperature is almost linear, as shown in Fig. 2, and the performance difference is within the error bar. The gap to the predicted performance, see [7] for discussion, is of the order of 0.1 K.

The current at which the voltage take-off occurs, i.e. the quench current I_q, is shown in Fig. 3. Above 38 kA $(\mathrm{PFIS_W})$ and 45 kA $(\mathrm{PFIS_{NW}})$, i.e. when the take-off is observed at very low electric field level, the behavior of I_q vs. T strongly deviates from linearity and the performance is much poorer than expected from the strand. Despite some scattering observed in the high current I_q results, the performance of $\mathrm{PFIS_{NW}}$ is

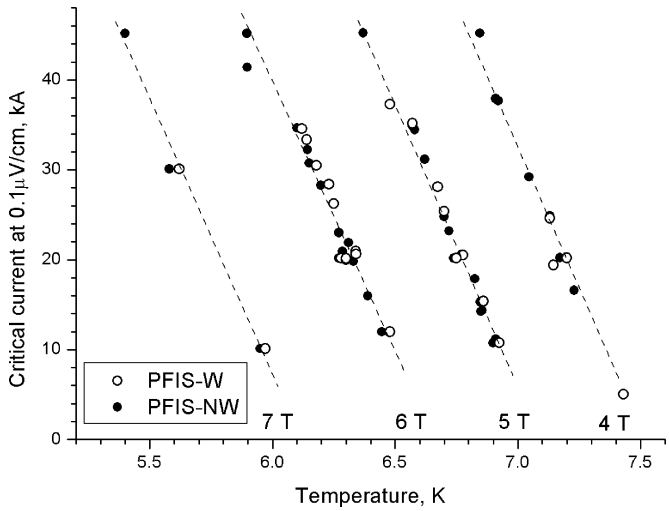

Fig. 2. Summary of critical current and current sharing temperature at the electrical field criterion 0.1 $\mu\mathrm{V}/\mathrm{cm}$ at background field of 4, 5, 6 and 7 T. The dashed lines are linear interpolations.

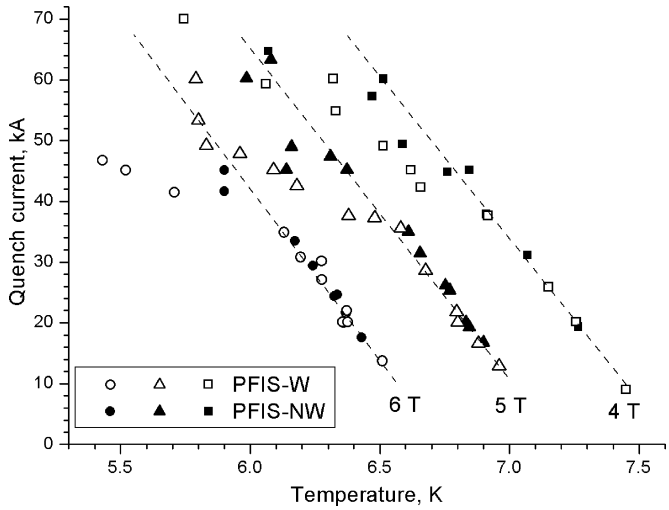

Fig. 3. Summary of quench current results from all the critical current and current sharing temperature runs at 4, 5 and 6 T. The dashed lines are linear interpolations for the low current range.

better than $\mathrm{PFIS_W}$, i.e. the deviation from linearity is smaller and occurs at higher current.

The large deviation from the linear behavior is not an intrinsic feature of the self-field induced quenches. To understand the behavior in Fig. 3, we must postulate some current unbalance among the strands. When enough voltage builds up along the strands, see I_c results in Fig. 2, current re-distribution from the overloaded strands is possible in both $\mathrm{PFIS_{NW}}$ and $\mathrm{PFIS_W}$. In the condition of self-field induced quench, i.e. with high local electric field but very low average voltage, the overloaded strands are unable to transfer the excess current to the neighboring strands and quench.

The better behavior of $\mathrm{PFIS_{NW}}$ suggests that the sub-cable wraps restrict the current re-distribution process. Indeed, for the same quench current, a higher $\mathrm{E_q}$ is observed at $\mathrm{PFIS_{NW}}$ compared to $\mathrm{PFIS_W}$ [13].

The ITER design values for T_cs of the PF1&6 conductor at 45 kA, 6 T peak field, is 6.5 K, i.e. 1.5 K above the operating

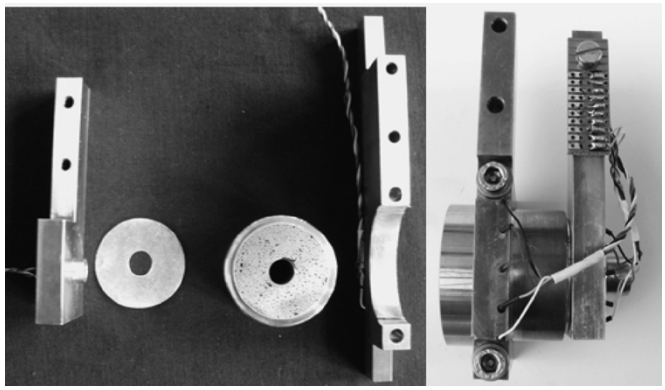

Fig. 4. The slice of conductor termination and its holder: exploded view (left) and assembled sample (right).

temperature of 5 K. The test conditions of the PFIS are not identical to ITER-PF: the self-field gradient is higher in the PFIS and the joint is closer to the high field. The NbTi strand fulfills the ITER spec at 4.2 K, but the J_c interpolated at higher temperature is lower than retained in ITER. On the other hand, the non-Cu cross section is 8% larger than in the ITER PF1&6 and the central channel is blocked.

Interpolating the experimental results, rescaled with the NbTi area with respect to the ITER coils, one gets a quench temperature of 5.80 K for $\mathrm{PFIS_W}$ and 6.05 K for $\mathrm{PFIS_{NW}}$ in the ITER PF1&6 coil normal operation, i.e. a temperature margin of only 0.80 K and 1.05 K for $\mathrm{PFIS_W}$ and $\mathrm{PFIS_{NW}}$, respectively. These values are also lower than those obtained on a previous sample (PF-FSJS), i.e. 1.25 K and 1.40 K for the left and right legs, respectively [14]. Such a result can be explained both by a lower strand performance [8] and by highly uneven current distributions among strands [7].

Compared to the short sample test in SULTAN, the performance of the insert coil (PFCI) will benefit of a less steep self-field gradient, a longer distance between joint and high field, a longer section exposed to high field and (hopefully) a better balanced current distribution from the joint. On the other hand, the central channel will be open.

B. Joint Resistance

The cable end for the upper termination of the PFIS, connecting to the SULTAN transformer, is prepared like the joint, with the Cu saddle replaced by a flat Cu plate.

An unexpected high resistance was observed in the joint (about 10 $\mathrm{n\Omega}$) and in the termination (about 6 $\mathrm{n\Omega}$ for $\mathrm{PFIS_{NW}}$ and 18 $\mathrm{n\Omega}$ for $\mathrm{PFIS_W}$).

The high resistivity of the CuCrZr sleeve, $\rho = 9.5 \cdot 10^{-9}\ \Omega\mathrm{m}$, makes up to 4 $\mathrm{n\Omega}$ of the joint resistance. The remainder is likely due to the cable-to-sleeve contact (Ag coated strands pressed/heated to the tinned inner wall of the sleeve).

A 28 mm long slice was cut by electronic erosion from a conductor termination, prepared in the same way as for the PFIS joint. The resistance of the slice was measured at CRPP in liquid helium, with the holder shown in Fig. 4. The result, $R_\mathrm{slice} = 240\ \mathrm{n\Omega}$ for a contact length of 10 mm, scales satisfactorily to $R_\mathrm{joint} = 2 \cdot R_\mathrm{slice}(10/450) = 10.6\ \mathrm{n\Omega}$, providing an easy

method to quickly assess the improvements that are planned at Tesla for the PFIC conductor termination [1], [2].

The maximum allowable resistance for the joints of the ITER PF coils is 5 $\mathrm{n}\Omega$ at 4 T, 45 kA [4]. Other full size NbTi joints for ITER have achieved resistance of $\approx 1.5\ \mathrm{n}\Omega$ (PF-FSJS [14]), and $\approx 0.7\ \mathrm{n}\Omega$ (CRPP low cost joint [15]).

C. AC Loss

The initial AC loss results of the PFIS were not satisfactory as the magnetization signals could not be properly balanced. Accurate calorimetric ac loss tests were carried out at a later campaign (after cyclic load) in the range of 0.2 to 4 Hz. The measured time constant $\mathrm{n}\tau$ is 9.5 ms and 20 ms respectively for $\mathrm{PFIS_W}$ and $\mathrm{PFIS_{NW}}$.

The ac loss results in SULTAN are in good agreement with the results obtained for the same conductors in the "press" facility at the University of Twente [16], after a similar number of load cycles.

D. Current Distribution

Opposite to other SULTAN tests, in which sensors from other supplier were used [17], for the PFIS Hall sensors placed in high field and close to the joints, with large parallel field component, a nonlinear response is observed for a small transverse field component. Applying a superimposed AC and background field, the Hall coefficient was re-calculated at the operating conditions.

During T_{cs} runs at small, constant operating current and slowly increasing temperature, a slow change in the response of the Hall sensors indicates a smooth current re-distribution, [13], [18]. A small, saw-tooth ripple of Hall sensors signals at T_{cs} runs with high operating current is correlated with voltage spikes. An interpretation, discussed in detail in [19], suggests the occurrence of local quenches and recovery.

At constant operating current, far from T_{cs}, the observed current unbalance is slightly larger in the conductor without wraps, but the extent of current re-distribution close to T_{cs} is also larger. The algorithms for current profile reconstruction must use models with a small number of current carrying elements. The Hall sensors arrays are of little help to solve the case of large current unbalance between neighboring strands.

IV. Conclusion

The conductor DC performances in the high current range appear to be heavily influenced by a nonuniform current distribution: the $\mathrm{PFIS_{NW}}$ shows a better behavior, probably due to its higher capacity to redistribute current. Nevertheless, the performance of both legs is below ITER specifications.

Both conductors, as already observed in [14], suffers of self-field induced take-offs and have no measurable T_{cs} at high current. The removal of sub-cable wraps helps to increase the threshold for instability. The electric field before take-off, E_{q}, is larger in $\mathrm{PFIS_{NW}}$.

The high joint resistance, $\approx 10\ \mathrm{n}\Omega$, is not acceptable for ITER coils. Improvements of joint layout are on going at Tesla for the PF Coil Insert. The high joint resistance and high current unbalance come likely both from the strand/copper interface problem in the joint.

In the SULTAN test, the AC loss is in the same range of typical NbTi strand loss, for both conductors, with and without wraps.

From the Hall sensors, valuable information can be drawn about the current unbalance and the ability to re-distribute the current.

Acknowledgment

The technical support of PSI in the experimental activity is acknowledged.

References

[1] R. Zanino *et al.*, "Preparation of the ITER Poloidal Field Conductor Insert (PFCI) test," *IEEE Trans. Appl. Supercond.*, vol. 15, no. 2, Jun. 2005.

[2] F. Hurd *et al.*, "Design and manufacture of a full size joint sample for the qualification of the Poloidal Field (PF) insert coil," *IEEE Trans. Appl. Supercond.*, vol. 15, no. 2, Jun. 2005.

[3] P. Bruzzone *et al.*, "Upgrade of operating range for SULTAN test facility," *IEEE Trans. Appl. Supercon.*, vol. 12, pp. 520–523, Mar. 2002.

[4] Magnet Superconducting and Electrical Design Criteria, ITER Final Design Report 2001: DRG1 Annex, IAEA, Vienna, 2001.

[5] Superconducting Cable of the ITER PF Conductor Insert, JSC VNIIKP, Quality Book V.QB01-05, Podolsk, 2001.

[6] G. Vedernikov *et al.*, "The study of critical current dependency on temperature and magnetic field for the NbTi strand intended for ITER PF insert coil," *IEEE Trans. Appl. Supercond.*, vol. 14, no. 2, pp. 1028–1031, Jun. 2004.

[7] D. Ciazynski *et al.*, "DC performances of ITER NbTi conductors: Models versus measurements," *IEEE Trans. Appl. Supercond.*, vol. 15, no. 2, Jun. 2005.

[8] L. Zani *et al.*, "$\mathrm{J_c(B, T)}$ characterization of NbTi strands used in the ITER poloidal field coil-relevant full scale joint samples and inserts," *IEEE Trans. Appl. Supercond.*, vol. 15, no. 2, Jun. 2005.

[9] User Specification for Conductor Samples to be Tested in the SULTAN Facility, CRPP LRP 723/02, Jun. 2002.

[10] P. Bruzzone, A. Formisano, and R. Martone, "Optimal magnetic probes location for current reconstruction in multistrands superconducting cables," *IEEE Trans. Mag.*, vol. 38, no. 2, pp. 1057–1060, Mar. 2002.

[11] Y. Ilyin *et al.*, "Reconstruction of the current unbalance in full-size ITER NbTi CICC by self field measurements," *IEEE Trans. Appl. Supercond.*, vol. 15, no. 2, Jun. 2005.

[12] R. Wesche *et al.*, "Self-field effects in NbTi subsize cable-in-conduit conductors," *Phys. C: Superconductivity*, vol. 401, pp. 113–117, Jan. 2004.

[13] R. Wesche *et al.*, "Analyses and implications of V-I characteristic of PF insert conductor sample," presented at the SOFT 2004, Venice, Italy, Sep. 2004.

[14] D. Ciazynski *et al.*, "Test results of the first 50 kA NbTi full size sample for ITER," *Supercond. Sci. Technol.*, vol. 17, pp. 155–160, May 2004.

[15] B. Stepanov *et al.*, "A low cost joint for the ITER PF coils, design and test results," presented at the SOFT 2004, Venice, Italy, Sep. 2004.

[16] Y. Ilyin *et al.*, "Effect of cyclic loading and conductor layout on contact resistance of full-size ITER PFCI conductors," *IEEE Trans. Appl. Supercond.*, vol. 15, no. 2, Jun. 2005.

[17] P. Bruzzone, A. Fuchs, B. Stepanov, and G. Vecsey, "Transient stability results for Nb3Sn cable-in-conduit conductors," *IEEE Trans. Appl. Supercond.*, vol. 12, no. 1, pp. 512–515, Mar. 2002.

[18] A. Formisano *et al.*, "DC and transient current distribution analysis from self-field measurements on ITER PFIS conductor," presented at the SOFT 2004, Venice, Italy, Sep. 2004.

[19] P. Bruzzone, B. Stepanov, and E. Zapretilina, "V-I characteristics with 'bumps' in the medium size NbTi CICC cables," presented at the SOFT 2004, Venice, Italy, Sep. 2004.